P H Y S I C A L   R E V I E W   L E T T E R S

Membrane Composition Variation and Underdamped Mechanics near Transmembrane Proteins and Coats

S. Alex Rautu,[1] George Rowlands,[1] and Matthew S. Turner[1,2,*]

[1]*Department of Physics, University of Warwick, Coventry CV4 7AL, United Kingdom*
[2]*Centre for Complexity Science, University of Warwick, Coventry CV4 7AL, United Kingdom*
(Received 8 July 2014; published 2 March 2015)

We study the effect of transmembrane proteins on the shape, composition, and thermodynamic stability of the surrounding membrane. When the coupling between membrane composition and curvature is strong enough, the nearby membrane composition and shape both undergo a transition from overdamped to underdamped spatial variation, well before the membrane becomes unstable in the bulk. This transition is associated with a change in the sign of the thermodynamic energy and, hence, favors the early stages of coat assembly necessary for vesiculation (budding) and may suppress the activity of mechanosensitive membrane channels and transporters. Our results suggest an approach to obtain physical parameters of the membrane that are otherwise difficult to measure.

Biological membranes are crucial to the structure and function of living cells [1]. Transmembrane proteins essential for transport, adhesion, and signaling are embedded in membranes [2,3] consisting of a mixture of lipids and other amphipathic components. The interaction with the adjacent lipid molecules is known to regulate the function of membrane proteins [4–7]. Here, we are primarily interested in the nonspecific lipid-protein interactions that arise from the coupling of their hydrophobic regions [8–14], although we can also allow for selective enrichment of membrane component(s) near the protein. We employ a continuum theory in which small deformations of the lipid environment near a rigid inclusion can be described by a number of local field variables, such as the profile of the midplane of the bilayer, its composition, and membrane thickness [15–36]. Furthermore, the free-energy cost associated with thickness deformation is completely decoupled at lowest order [21], and it can be independently analyzed, although we do not do so here.

We allow for selective enrichment or depletion of curvature-sensitive inclusions in the vicinity of a membrane protein or, equivalently, lipid asymmetry between leaflets that is characterized by a local spontaneous curvature, the preferred mean curvature in the absence of any mechanical stresses on the membrane [33–41]. This local variation may be relatively large near a membrane protein if its geometry is such that it bends or deforms the surrounding membrane (see Fig. 1). Our approach leads to a real-space description of the membrane around an inclusion of arbitrary symmetry.

We consider a two-component membrane in which the local compositional asymmetry between the different layers and/or the density of curvature-sensitive inclusions is phenomenologically coupled to the local mean curvature of the membrane [33,34]. When the compositional variation is weak and the membrane displacement is small, the free energy can be written as a Landau-Ginzburg expansion [33–35,42–44],

$$\mathcal{F}_\varphi = \frac{1}{2} \int_\mathcal{M} [a\varphi^2 + b(\nabla\varphi)^2 + 2c\varphi(\nabla^2 u)]d^2\mathbf{r}, \quad (1)$$

where only the lowest-order terms are retained and a, b, and c are phenomenological constants. The scalar fields $\varphi(\mathbf{r})$ and $u(\mathbf{r})$ are the local composition difference (as an area fraction) and bilayer midplane height, respectively; see Fig. 1. Both deformation fields are described within a Monge representation, which allows us to write the free energy associated with midplane deformation as

$$\mathcal{F}_u = \frac{1}{2} \int_\mathcal{M} [\sigma(\nabla u)^2 + \kappa(\nabla^2 u)^2]d^2\mathbf{r}, \quad (2)$$

where σ and κ are the surface tension and bending rigidity of the membrane, respectively [45].
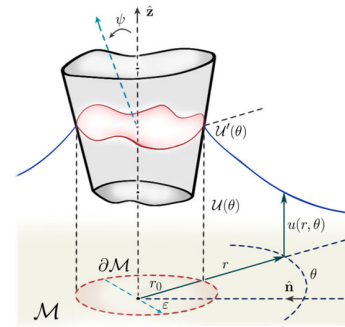

FIG. 1 (color online). Sketch of a membrane inclusion showing the midplane of the bilayer (blue line) at height $u(r, \theta)$. The surface variation of the rigid inclusion in the $\hat{\mathbf{z}}$ direction is coarse grained out so that the geometry is defined by its radius r_0 and two functions describing the height $\mathcal{U}(\theta)$ and contact angle $\mathcal{U}'(\theta)$ of the hydrophobic belt. These parametrize the protein-membrane interface (red line), where $u(r_0, \theta) = \mathcal{U}(\theta)$ and $\hat{\mathbf{n}} \cdot \nabla u(r_0, \theta) = \mathcal{U}'(\theta)$, with $\hat{\mathbf{n}}$ as the inward unit normal vector. We require both the normal force and the torque on the inclusion to vanish. The latter can lead to an equilibrium tilt angle ψ about the axis labeled by ε.

We now seek the ground state of the membrane and neglect fluctuations throughout. The membrane shape $u(\mathbf{r})$ and its compositional field $\varphi(\mathbf{r})$ can then be computed exactly by minimizing the free-energy functional $\mathcal{F} = \mathcal{F}_u + \mathcal{F}_\varphi$, leading to the Euler-Lagrange equations

$$\nabla^2 u = (\nabla^2 - \beta^2)\phi, \tag{3}$$

$$\nabla^2(\nabla^2 - \alpha^2)u + \gamma^2\nabla^2\phi = 0, \tag{4}$$

where $\phi(\mathbf{r}) = (b/c)\varphi(\mathbf{r})$ and the coefficients $\alpha = \sqrt{\sigma/\kappa}$, $\beta = \sqrt{a/b}$, and $\gamma = c/\sqrt{\kappa b}$ represent the relevant inverse length scales of the model [46]. By combining Eqs. (3) and (4), a single equation for $\phi(\mathbf{r})$ can be obtained (Supplemental Material [47]),

$$(\nabla^2 - k_+^2)(\nabla^2 - k_-^2)\phi = 0, \tag{5}$$

where $k_\pm$ is given by

$$k_\pm = \frac{1}{2}\left[\sqrt{(\alpha+\beta)^2 - \gamma^2} \pm \sqrt{(\alpha-\beta)^2 - \gamma^2}\right]. \tag{6}$$

By separation of variables, a solution to Eq. (5) that vanishes in the far-field limit can be found to be

$$\phi(r,\theta) = \phi_+(r,\theta) + \phi_-(r,\theta), \tag{7}$$

where r and θ are the usual polar coordinates, as illustrated in Fig. 1, and $\phi_\pm$ is defined by

$$\phi_\pm(r,\theta) = \frac{k_\pm^2}{k_\pm^2 - \beta^2}\sum_{n=0}^{\infty}\mathcal{V}_n^\pm(\theta)K_n(k_\pm r), \tag{8}$$

where K_n are the modified Bessel functions of the second kind of order n, and $\mathcal{V}_n^\pm(\theta) = \mathcal{A}_n^\pm\cos(n\theta) + \mathcal{B}_n^\pm\sin(n\theta)$, with $\mathcal{A}_n^\pm$ and $\mathcal{B}_n^\pm$ arbitrary constants. From this, we obtain the membrane shape through Eq. (3), which yields

$$u(r,\theta) = u_+(r,\theta) + u_-(r,\theta) + u_h(r,\theta), \tag{9}$$

where the solutions that diverge at infinity are excluded. Here, $u_h(r,\theta)$ is the homogeneous solution of Eq. (3), namely,

$$u_h(r,\theta) = \sum_{n=0}^{\infty}\mathcal{W}_n(\theta)r^{-n}, \tag{10}$$

where $\mathcal{W}_n(\theta) = \mathcal{X}_n\cos(n\theta) + \mathcal{Y}_n\sin(n\theta)$, with $\mathcal{X}_n$ and $\mathcal{Y}_n$ some constants. The remaining two terms in Eq. (9) are the inhomogeneous solutions, which are found to be

$$u_\pm(r,\theta) = \sum_{n=0}^{\infty}\mathcal{V}_n^\pm(\theta)K_n(k_\pm r). \tag{11}$$

The angular functions $\mathcal{V}_n^\pm(\theta)$ and $\mathcal{W}_n(\theta)$ are determined by the boundary conditions at the interface $\partial\mathcal{M}$, located at a distance r_0 from the symmetry axis. These are specified by the height $\mathcal{U}(\theta)$ and contact angle $\mathcal{U}'(\theta)$ at which the midplane of the bilayer meets the inclusion (see Fig. 1). This choice is motivated by assuming a strong coupling between the transmembrane domain of the inclusion and the membrane hydrophobic core. Also, the normal

derivative of ϕ is chosen to vanish on $\partial\mathcal{M}$, which is used to obtain a unique solution [51].

This methodology allows us to compute exactly the lowest order estimates to the membrane profile, its local phase behavior, and the total deformation energy, given an arbitrary model for the shape of the inclusion, through $\mathcal{U}(\theta)$ and $\mathcal{U}'(\theta)$, i.e., a general solution to the problem. This makes contact with experiments that might measure membrane shape (cryo TEM [52] or perhaps TIRF microscopy) and composition (NMR [53] or FRET [54]). First, we consider a simple illustrative example in which the height $\mathcal{U}(\theta)$ is chosen to be a constant z_0, while the contact angle has a nonzero value only within an angular interval w; see Fig. 2. This corresponds to a rigid inclusion that induces a local midplane deformation only within a specific region along its hydrophobic belt, with the remaining part preferring a flat membrane. The Connolly surface of a leucine transporter, LeuT, exhibits similar features [55,56]. The height z_0 is not entirely arbitrary, being set by the overall balance of normal forces. Similarly, the condition of torque balance leads to a tilt of the inclusion (see the Supplemental Material [47] for details), as illustrated in Fig. 1. Typical solutions due to such an asymmetrically shaped inclusion that exerts no net torque are shown in Fig. 2 for physiologically reasonable values of α, β, and γ [57]. The induced $\phi(\mathbf{r})$ values show a rich variation as the angle w is varied between 0 and 2π, which correspond to inclusions with a cylindrical and a conical shape, respectively.

To better understand the role of the coupling constant γ, we consider symmetric conical inclusions ($w = 2\pi$) in what
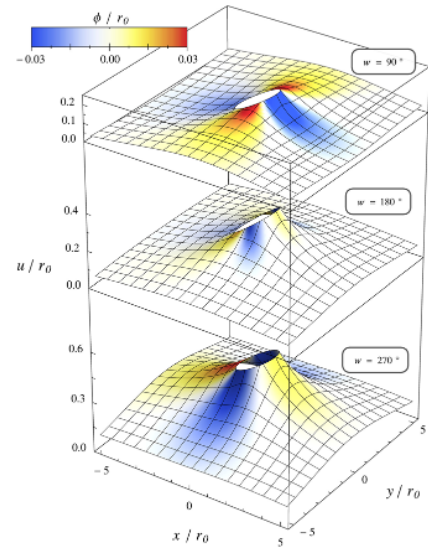

FIG. 2 (color online). Membrane profiles induced by an asymmetrical inclusion, where the contact angle is given by $\mathcal{U}'(\theta) = 15°$ if $|\theta| < w/2$ and 0 otherwise, with θ measured from the x axis (see text). The membrane parameters are here $\alpha r_0 = 0.1$, $\beta r_0 = 1.0$, and $\gamma r_0 = 0.5$, with r_0 the radius of the inclusion (not depicted). The compositional asymmetry $\phi(\mathbf{r})$ is shown as the color map of the surface plots.

follows, noting that the transition from over- to under-damped variation also appears for rigid inclusions with other (or no) symmetry. For values of γ less than $\gamma_d = |\alpha - \beta|$, the solutions are found to be monotonically decaying; see Fig. 3(b). However, as γ is increased above this point, the solutions show an underdamped behavior, with the membrane displacement decaying to zero for large distances. The magnitude of this amplitude becomes large as γ approaches $\gamma_c = \alpha + \beta$, suggesting the presence of an instability. In fact, $\gamma > \gamma_c$, where $k_\pm^2 < 0$ as shown in Fig. 3(a), corresponds to Leibler's criterion for curvature-induced instabilities in (bulk) membranes [33,34]. The point $\gamma = \gamma_d$ instead corresponds to a critically damped system, separating the real and complex domain of $k_\pm$. The solutions are thermodynamically stable on either side of this boundary. When $\gamma_d < \gamma < \gamma_c$, the decay rate λ of the membrane undulations and its wave number ω can be determined by approximating $K_n(\rho) \approx e^{-\rho}(\pi\rho/2)^{-1/2}$ for $\rho \gg n$ in Eq. (9) [61], i.e.,

$$u(r) \sim \frac{e^{-\lambda(r-r_0)}}{\sqrt{r/r_0}} \cos\left[\omega(r - r_0) + \vartheta\right], \qquad (12)$$

where ϑ is a phase angle that only depends on α, β, and γ. Here, λ and ω are given by the real and imaginary parts of Eq. (6), respectively. Thus, we find that the wavelength of the precritical undulations diverges as we approach $\gamma = \gamma_d$, and the decay length diverges for $\gamma = \gamma_c$, which signals the presence of a bulk membrane instability. Physically and
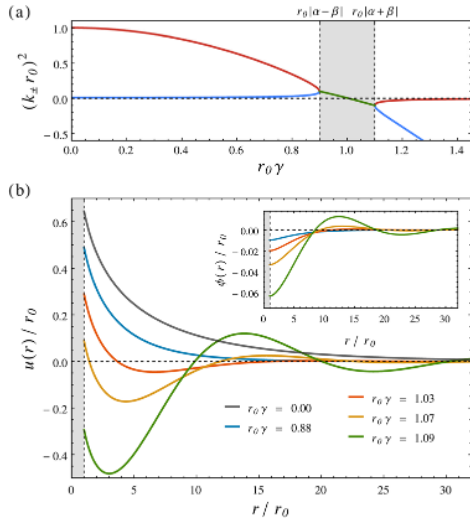

FIG. 3 (color online). (a) Plot of $k_\pm^2$ from Eq. (6) against the coupling constant γ, with $\alpha r_0 = 0.1$, $\beta r_0 = 1.0$, and r_0 the inclusion radius. This illustrates that both k_+ (red line) and k_- (blue line) are real for $\gamma < |\alpha - \beta|$ and purely imaginary when $\gamma > \alpha + \beta$. The gray shaded area illustrates the region where $k_\pm^2$ are complex, while the green line shows the real part only. The domain given by $\gamma > \alpha + \beta$ corresponds to Leibler's unstable regime [33,34]. (b) Radial profiles of the bilayer midplane $u(r)$ and the compositional asymmetry $\phi(r)$ induced by a conical inclusion, with a modest contact angle of 15°, for different values of the coupling constant γ, where α and β have the same values as those in panel (a).

mathematically distinct underdamped solutions have also been found in studies of membrane thickness mismatch without any compositional field that couples to midplane curvature [17].

While α can be measured through various experimental techniques [62–65], the parameters β and γ are more elusive [51]. Our analysis suggests a possible method to measure them, e.g., by tuning the system to lie near the instability threshold $\gamma \lesssim \gamma_c$. Here, the amplitudes of the undulations are large and long ranged, and γ and β can be inferred by comparison with Eqs. (9) or (12). This tuning might be achieved by controlling the surface tension, e.g., using a micropipette aspiration technique [62], so as to approach the critical tension $\sigma_c = \kappa(\gamma - \beta)^2$, although the presence of thermal fluctuations may mean that some averaging will be required to resolve the ground state, particularly far from the membrane inclusion. This illustrates the predictive power of our model.

Mechanosensitive membrane channels have been widely studied and reveal the interplay between the biological function of transmembrane proteins and the adjacent membrane structure and composition. Through conformational changes from a closed to an open state that allows the passage of solvent through the membrane, they can equilibrate an osmotic imbalance between the interior and the exterior of cells [66–68]. Although many examples of these channels are found in nature, the bacterial mechanosensitive channels of large (MscL) and small conductance (MscS) are prototypes of such proteins. Experimental studies have have shown that the channel opening probability is related to the membrane tension and the size of the open pore [66–73]. One possibility is that the channel simply dilates open at high tension, but the transition between the closed and open states might also involve, e.g., a change in slope at the protein-membrane interface (here, δ) [74]. In a two-component membrane such a change in boundary conditions between the closed and open states couples to both the shape and asymmetry field in the nearby membrane and hence contributes to a change in the free energy of the channel-membrane system. Here, for simplicity, we consider the angle at the channel wall δ to be nonzero in a conical closed state and $\delta = 0$ in the open state. We explore the thermodynamic effect of this gating by tilt by comparing the deformation energy $\mathcal{F}$ of the membrane to the experimental estimate of the energy required to open the channels at zero tension, inferred by assuming a purely dilational opening. Figure 4(a) shows that the even modest changes in the boundary angle at the face of the channel could give rise to a significant thermodynamic energy under gating by tilt. Moreover, a regime is identified in which the membrane can act to *close*, rather than open, the channel, characterized by a negative total energy $\mathcal{F}$ relative to the open state, although a similar result was previously identified in a model that neglects spatial variation of coupling to curvature [23,24]. Our results indicate that lipid composition variation and its coupling to mean curvature could play a role in regulating the function of mechanosensitive membrane channels.
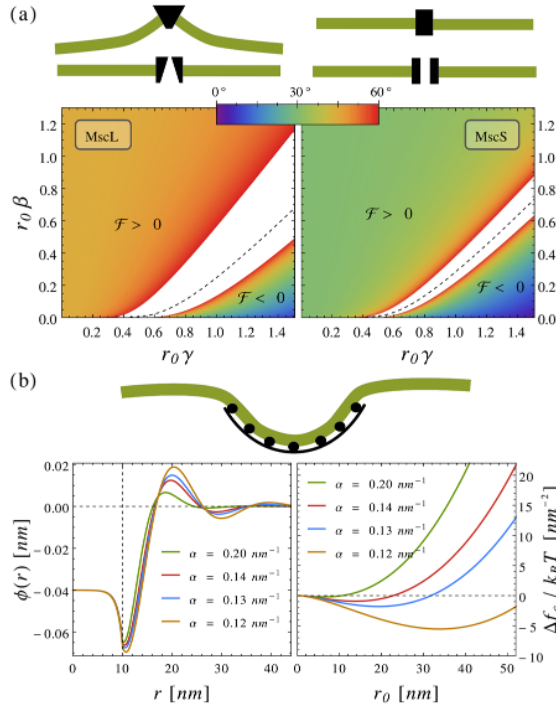
FIG. 4 (color online). (a) The top sketches, with the bilayer membrane represented by a thick green line, show two idealized schemes for channel gating: the gating-by-tilt model (left) and the dilational gating model (right). The figures below this show the angle for gating by tilt that would account for the absolute value of the *entire* conformational energy change $\mathcal{F}$ measured for MscL and MscS [69,70]. The dashed line indicates $\mathcal{F} = 0$ separating two domains where the membrane acts to open ($\mathcal{F} > 0$) or close ($\mathcal{F} < 0$) the gating channel. The uncolored region is not shown, as it corresponds to angles greater than 60°, which are probably unphysical and where our perturbative approach anyway breaks down. (b) The top sketch shows a membrane deformed by the assembly of a protein coat such as clathrin or a viral coat protein. The graphs below this show the radial compositional field $\phi(r)$ when the coat is of size $r_0 = 10$ nm (left) and the change in membrane energy per area of coat monomers $\triangle f_c$ due to coupling to the composition field against the coat radius r_0 (right). In both cases, we assume a typical intrinsic coat curvature with $\mathcal{R}_c = 50$ nm, $\beta = 1.0$ nm^{-1}, and $\gamma = 1.1$ nm^{-1}. In the underdamped regime, the energy change $\triangle f_c$ can exhibit an initial decrease, which may drive coat assembly. In both (a) and (b) we use $\kappa = 20 k_B T$.

Finally, the presence of a negative deformation energy in the underdamped regime motivated us to study the thermodynamics of protein coat formation on a membrane. Such coats are important in regulation, e.g., membrane trafficking using clathrin coats, or in infection, where viral coats assemble at the plasma membrane [1]. Figure 4(b) shows both the compositional field ϕ around a protein coat of size $r_0 = 10$ nm and the variation with r_0 of $\triangle f_c$, i.e., the change in membrane energy due to coupling to ϕ only, scaled by the coat area. Thus, $\triangle f_c$ renormalizes the chemical potential for binding of early coat monomers to the membrane, and it is computed by adding both the contribution from the

membrane inside (under) and outside the coat (Supplemental Material [47]). Two striking features are observed in the underdamped regime. First, this free-energy change can support an initial *decrease* with coat size. In this case, the deformation of the membrane (with its associated composition) is energetically favorable. This is true (even) for membranes that remain thermodynamically stable, i.e., in the absence of bulk instability. This may represent a new mechanism for driving (controlling) coat formation in cells. This might be tested by tracking coat assembly at different α (tension), e.g., controlled by micropipette aspiration [62]: We predict a dramatic increase in the rate of assembly near the critical tension σ_c. Second, the existence of a minimum in $\triangle f_c$ corresponds to a characteristic coat size with metastable character; we note that partially formed coats are often observed [75].

*Corresponding author.
m.s.turner@warwick.ac.uk

[1] B. Alberts, A. Johnson, J. Lewis, M. Raff, K. Roberts, and P. Walter, *Molecular Biology of the Cell*, 5th ed. (Garland Science, New York, 2008).
[2] S. J. Singer and G. L. Nicolson, Science **175**, 720 (1972).
[3] D. M. Engelman, Nature (London) **438**, 578 (2005).
[4] T. M. Suchyna, S. E. Tape, R. E. Koeppe, O. S. Andersen, F. Sachs, and P. A. Gottlieb, Nature (London) **430**, 235 (2004).
[5] P. Moe and P. Blount, Biochemistry **44**, 12239 (2005).
[6] D. Krepkiy, M. Mihailescu, J. A. Freites, E. V. Schow, D. L. Worcester, K. Gawrisch, D. J. Tobias, S. H. White, and K. J. Swartz, Nature (London) **462**, 473 (2009).
[7] M. Milescu, F. Bosmans, S. Lee, A. A. Alabi, J. I. Kim, and K. J. Swartz, Nat. Struct. Biol. **16**, 1080 (2009).
[8] A. G. Lee, Biochim. Biophys. Acta **1666**, 62 (2004).
[9] K. Mitra, I. Ubarretxena-Belandia, T. Taguchi, G. Warren, and D. M. Engelman, Proc. Natl. Acad. Sci. U.S.A. **101**, 4083 (2004).
[10] W. Dowhan, E. Mileykovskaya, and M. Bogdanov, Biochim. Biophys. Acta **1666**, 19 (2004).
[11] T. K. M. Nyholm, S. Ozdirekcan, and J. A. Killian, Biochemistry **46**, 1457 (2007).
[12] O. S. Andersen and R. E. Koeppe, Annu. Rev. Biophys. Biomol. Struct. **36**, 107 (2007).
[13] R. Phillips, T. Ursell, P. Wiggins, and P. Sens, Nature (London) **459**, 379 (2009).
[14] J. A. Lundbaek, S. A. Collingwood, H. I. Ingólfsson, R. Kapoor, and O. S. Andersen, J. R. Soc. Interface **7**, 373 (2010).
[15] P. B. Canham, J. Theor. Biol. **26**, 61 (1970).
[16] H. W. Huang, Biophys. J. **50**, 1061 (1986).
[17] H. Aranda-Espinoza, A. Berman, N. Dan, P. Pincus, and S. A. Safran, Biophys. J. **71**, 648 (1996).
[18] C. Nielsen, M. Goulian, and O. S. Andersen, Biophys. J. **74**, 1966 (1998).

[19] S. Mondal, G. Khelashvili, and H. Weinstein, Biophys. J. **106**, 2305 (2014).

[20] P. Sens and S. Safran, Eur. Phys. J. E **1**, 237 (2000).

[21] J.-B. Fournier, Eur. Phys. J. B **11**, 261 (1999).

[22] T. R. Weikl, M. M. Kozlov, and W. Helfrich, Phys. Rev. E **57**, 6988 (1998).

[23] P. Wiggins and R. Phillips, Proc. Natl. Acad. Sci. U.S.A. **101**, 4071 (2004).

[24] P. Wiggins and R. Phillips, Biophys. J. **88**, 880 (2005).

[25] N. Dan, P. Pincus, and S. A. Safran, Langmuir **9**, 2768 (1993).

[26] M. Goulian, R. Bruinsma, and P. Pincus, Europhys. Lett. **22**, 145 (1993).

[27] K. S. Kim, J. Neu, and G. Oster, Biophys. J. **75**, 2274 (1998).

[28] M. S. Turner and P. Sens, Biophys. J. **76**, 564 (1999).

[29] V. S. Markin and F. Sachs, Phys. Biol. **1**, 110 (2004).

[30] T. Ursell, K. C. Huang, E. Peterson, and R. Phillips, PLoS Comput. Biol. **3**, e81 (2007).

[31] C. A. Haselwandter and R. Phillips, Europhys. Lett. **101**, 68002 (2013).

[32] C. A. Haselwandter and R. Phillips, PLoS Comput. Biol. **9**, e1003055 (2013).

[33] S. Leibler, J. Phys. (Les Ulis, Fr.) **47**, 507 (1986).

[34] S. Leibler and D. Andelman, J. Phys. (Les Ulis, Fr.) **48**, 2013 (1987).

[35] D. Andelman, T. Kawakatsu, and K. Kawasaki, Europhys. Lett. **19**, 57 (1992).

[36] W. Helfrich, Z. Naturforsch. C **28**, 693 (1973).

[37] U. Seifert, Adv. Phys. **46**, 13 (1997).

[38] J. N. Israelachvili, D. J. Mitchell, and B. W. Ninham, J. Chem. Soc., Faraday Trans. **72**, 1525 (1976).

[39] S. M. Gruner, J. Phys. Chem. **93**, 7562 (1989).

[40] H. T. McMahon and J. L. Gallop, Nature (London) **438**, 590 (2005).

[41] A. Callan-Jones, B. Sorre, and P. Bassereau, Cold Spring Harbor Persp. Biol. **3**, a004648 (2011).

[42] P. B. Sunil Kumar, G. Gompper, and R. Lipowsky, Phys. Rev. E **60**, 4610 (1999).

[43] M. Schick, Phys. Rev. E **85**, 031902 (2012).

[44] U. Seifert, Phys. Rev. Lett. **70**, 1335 (1993).

[45] D. Nelson, T. Piran, and S. Weinberg, *Statistical Mechanics of Membranes and Surfaces*, 2nd ed. (World Scientific Publishing Company, Singapore, 2004).

[46] The sign choice of γ is simply a convention. The fields u and ϕ are invariant under a sign change in γ, itself related to the convention of a direction for "up" and whether one refers to the enrichment of a component that couples to positive curvature (depending on one's choice for up) or the depletion of one that couples to negative curvature.

[47] See Supplemental Material at http://link.aps.org/supplemental/10.1103/PhysRevLett.114.098101, which includes Refs. [48–50], for supporting calculations, including equations for the membrane shape and composition, curvature instability, and analysis of protein coat energetics.

[48] K. F. Riley, M. P. Hobson, and S. J. Bence, *Mathematical Methods for Physics and Engineering*, 3rd ed. (Cambridge University Press, Cambridge, England, 2006).

[49] F. W. Byron and R. W. Fuller, *The Mathematics of Classical and Quantum Physics* (Dover Publications Inc., New York, 1992).

[50] I. S. Gradshteyn, I. M. Ryzhik, A. Jeffrey, and D. Zwillinger, *Table of Integrals, Series, and Products*, 6th ed. (Academic Press, New York, 2000).

[51] Although Dirichlet boundary conditions could be used as well, our choice gives the ground state solution in the absence of any constraints on the composition asymmetry field ϕ at the boundary; see Supplemental Material [47] for more details.

[52] A. Shimada, H. Niwa, K. Tsujita, S. Suetsugu, K. Nitta, K. Hanawa-Suetsugu, R. Akasaka, Y. Nishino, M. Toyama, L. Chen, Z.-J. Liu, B.-C. Wang, M. Yamamoto, T. Terada, A. Miyazawa, A. Tanaka, S. Sugano, M. Shirouzu, K. Nagayama, T. Takenawa, and S. Yokoyama, Cell **129**, 761 (2007).

[53] P. J. Judge and A. Watts, Curr. Opin. Chem. Biol. **15**, 690 (2011).

[54] L. M. S. Loura and M. Prieto, Front. Psychol. **2**, 82 (2011).

[55] A. Yamashita, S. K. Singh, T. Kawate, Y. Jin, and E. Gouaux, Nature (London) **437**, 215 (2005).

[56] S. K. Singh, C. L. Piscitelli, A. Yamashita, and E. Gouaux, Science **322**, 1655 (2008).

[57] Typically, the membrane correlation length might be $\alpha^{-1} \sim 10\ r_0$ [58]. Equation (1) can be associated with a typical interfacial width for a strongly segregated system of a few nm, say $\sqrt{b/|a|} \sim r_0$, and a line tension of about a pN ($\sqrt{b|a|} \sim$ pN) [59], which combine to give $b \sim k_B T$. Sorting of strongly curvature-coupling components into membrane tubes gives an upper bound of $c \sim \kappa/(2.5 r_0)$ and, hence, a value for $\gamma \sim 2/r_0$ [60], indicating that all the regimes discussed in the main text are accessible. While the use of a phase-separated system to estimate the parameters a and b is questionable, given that they are motivated within a model in which the system remains essentially one phase, with ϕ very small, we are reassured that the primary limit on the accessibility of the underdamped regime is that β is not too large. Given that spontaneous phase separation is often seen on biological membranes, there would seem to be no lower limit on a reasonable magnitude for a and hence β.

[58] M. P. Sheetz and J. Dai, Trends Cell Biol. **6**, 85 (1996).

[59] A. Tian, C. Johnson, W. Wang, and T. Baumgart, Phys. Rev. Lett. **98**, 208102 (2007).

[60] S. Aimon, A. Callan-Jones, A. Berthaud, M. Pinot, G. E. S. Toombes, and P. Bassereau, Dev. Cell **28**, 212 (2014).

[61] M. Abramowitz and I. A. Stegun, *Handbook of Mathematical Functions* (Dover Publications Inc., New York, 1965).

[62] E. Evans and W. Rawicz, Phys. Rev. Lett. **64**, 2094 (1990).

[63] L. Bo and R. Waugh, Biophys. J. **55**, 509 (1989).

[64] M. Kummrow and W. Helfrich, Phys. Rev. A **44**, 8356 (1991).

[65] J. Pécréaux, H.-G. Döbereiner, J. Prost, J.-F. Joanny, and P. Bassereau, Eur. Phys. J. E **13**, 277 (2004).

[66] E. Perozo, Nat. Rev. Mol. Cell Biol. **7**, 109 (2006).

[67] I. R. Booth, M. D. Edwards, S. Black, U. Schumann, and S. Miller, Nat. Rev. Microbiol. **5**, 431 (2007).

[68] E. S. Haswell, R. Phillips, and D. C. Rees, Structure **19**, 1356 (2011).

[69] C.-S. Chiang, A. Anishkin, and S. Sukharev, Biophys. J. **86**, 2846 (2004).

[70] S. Sukharev, Biophys. J. **83**, 290 (2002).

[71] S. I. Sukharev, P. Blount, B. Martinac, F. R. Blattner, and C. Kung, Nature (London) **368**, 265 (1994).

[72] C. Kung, B. Martinac, and S. Sukharev, Annu. Rev. Microbiol. **64**, 313 (2010).

[73] E. Perozo, A. Kloda, D. M. Cortes, and B. Martinac, Nat. Struct. Biol. **9**, 696 (2002).

[74] M. S. Turner and P. Sens, Phys. Rev. Lett. **93**, 118103 (2004).

[75] J. Heuser, J. Cell Biol. **84**, 560 (1980).